J|A|C|S
COMMUNICATIONS

Published on Web 12/31/2005

Photoresponsive Multilayer Spiral Nanotubes: Intercalation of Polyfluorinated Cationic Azobenzene Surfactant into Potassium Niobate

Zhiwei Tong,[†] Shinsuke Takagi,[‡] Tetsuya Shimada,[‡] Hiroshi Tachibana,[‡] and Haruo Inoue*[,‡,§]

Department of Chemical Engineering, Huaihai Institute of Technology, Lianyungang, People's Republic of China, Department of Applied Chemistry, Graduate Course of Engineering, Tokyo Metropolitan University 1-1 Minami-ohsawa, Hachiohji-city, Tokyo 192-0397, Japan, and CREST, Japan Science and Technology (JST)

Received September 26, 2005; E-mail: inoue-haruo@c.metro-u.ac.jp

We will report here the first successful synthesis of photoresponsive multilayer spiral nanotubes by the introduction of polyfluorinate cationic azobenzene derivative, *trans*-[2-(2,2,3,3,4,4,4-heptafluorobutylamino)ethyl]-{2-[4-(4-hexyphenylazo)-phenoxy]-ethyl}dimethylammonium (abbreviated as C_3F_7-Azo^+), into layered niobate interlayer I by a two-step guest−guest exchange method using the intercalation compound, methyl viologen (MV^{2+})-$K_4Nb_6O_{17}$, as precursor.

Nanoscale tubular materials have attracted much attention due to their potential applications in optoelectronics, biosensors, catalysis, drug delivery, electrochemical energy production, and the separation of chiral compounds.[1] Because of their unique structural characteristics, the preparation of nanotubes is relatively difficult, and fewer synthetic techniques have been developed compared to those for other one-dimensional nanostructures, such as nanorods and nanowires.[2] Currently, there are two major methods for preparing nanotubes: template-assisted and nontemplate-assisted approaches. Template-assisted approaches mainly utilize a template to induce or confine the crystal growth of one-dimensional hollow nanostructures.[3] Nontemplate-assisted approaches usually exploit the proper control of reaction conditions to achieve nanotubes.[4] The nanotubes have been prepared by arc discharge, laser vaporization, and chemical vapor deposition. In all these approaches, high temperature is usually required. Recently, Mallouk et al. have reported the synthesis of niobate-based nanotubes at low temperature by exfoliation of acid-exchanged $K_4Nb_6O_{17}$ with tetra(*n*-butyl)-ammonium hydroxide in aqueous solution.[5] The interlayer space in the nanotubes was fixed and close to the original spacing in the $K_4Nb_6O_{17}$ crystals.

These reports prompted us to examine a preparation of novel photoresponsive multilayer nanotubes formed by the introduction of polyfluorinated cationic azobenzene derivative and cis−trans photoisomerization behavior of polyfluorinated cationic azobenzene C_3F_7-Azo^+ (see Supporting Information) in the interlayer space of multilayer spiral nanotubes. When methyl viologen (MV^{2+})-intercalated niobate was adopted as a precursor, the polyfluorinated C_3F_7-Azo^+ induced almost quantitative formation of spiral nanotubes from exfoliated nanosheets of niobate by rolling up with a sandwiched microstructure. The spiral nanotubes exhibited a swift photoresponse.

Polyfluorinated organic compounds are a unique class of organic compounds and have been the subject of recent research activity.[6] Their very weak intermolecular interactions with other molecules can be exploited for various applications. We have recently found that the ammonium cation-type polyfluorinated surfactants are easily intercalated into the clay interlayer spaces of sodium saponite to form rigidly packed bilayer structures.[7]

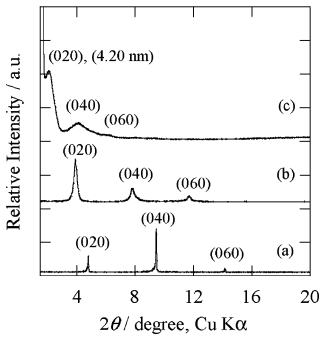

Figure 1. XRD patterns of the (a) $K_4Nb_6O_{17}\cdot 3H_2O$, (b) MV^{2+}-$K_4Nb_6O_{17}$, and (c) C_3F_7-Azo^+-$K_4Nb_6O_{17}$ hybrid nanotubes.

$K_4Nb_6O_{17}\cdot 3H_2O$ contains octahedral [NbO_6] units forming an anionic sheet disposed in a stacking arrangement.[8] The charge balance is maintained by the presence of potassium ions between the layers. $K_4Nb_6O_{17}\cdot 3H_2O$ has an orthorhombic unit cell with dimensions $a = 7.85$ Å, $b = 37.67$ Å, and $c = 6.64$ Å, containing two layers in the *b*-axis. It has two diffferent types of interlayer spaces (interlayers I and II) alternately between $[Nb_6O_{17}]^{-4}$ layers. Interlayer I contains potassium ions with water molecules, while interlayer II contains unhydrated potassium ions under ambient conditions.[9] The two types of interlayers exhibit different intercalating capabilities. The monovalent cations were intercalated into both the interlayers, and di- and trivalent cations were exchanged with the potassium ions in interlayer I only.[10]

The $K_4Nb_6O_{17}\cdot 3H_2O$ employed here was prepared by heating a 2.1:3.0 molar mixture of K_2CO_3 and Nb_2O_5 at 1100 °C for 10 h, following the procedures reported by Nassau et al.[9] The obtained powder was then identified by powder X-ray diffraction analysis and compared with existing crystallographic data (Figure 1a). A typical SEM image of the $K_4Nb_6O_{17}\cdot 3H_2O$ shows two-dimensional niobate sheets in a parallel layered structure (see Supporting Information). The intercalation compounds of $K_4Nb_6O_{17}$ with polyfluorinated cationic azobenzene (C_3F_7-Azo^+) could not be prepared by a direct intercalation reaction. MV^{2+}-$K_4Nb_6O_{17}$ intercalation compounds were used as the precursor. The intercalation of MV^{2+} ions into $K_4Nb_6O_{17}$ was carried out by treating $K_4Nb_6O_{17}\cdot 3H_2O$ with an aqueous solution of excess methyl viologen chloride ($MV^{2+}Cl_2$), then allowed to stand for three weeks at 70 °C. The intercalation of MV^{2+} into the hybrid was comfirmed by X-ray diffraction analysis (Figure 1b). The final multilayer spiral nanotubes C_3F_7-Azo^+-$K_4Nb_6O_{17}$ were prepared by the guest−guest ion exchange of MV^{2+}-$K_4Nb_6O_{17}$ with excess C_3F_7-Azo^+ in a glass ampule for two weeks at 70 °C. The multilayer spiral nanotubes C_3F_7-Azo^+-$K_4Nb_6O_{17}$ were confirmed by X-ray diffraction analysis (Figure 1c), atomic force microscope (AFM) images (Figure 2a,b), and high-resolution transmission electron microscope (HRTEM) image analysis (Figure 2c,d).

[†] Huaihai Institute of Technology.
[‡] Tokyo Metropolitan University.
[§] JST.

10.1021/ja0564564 CCC: $33.50

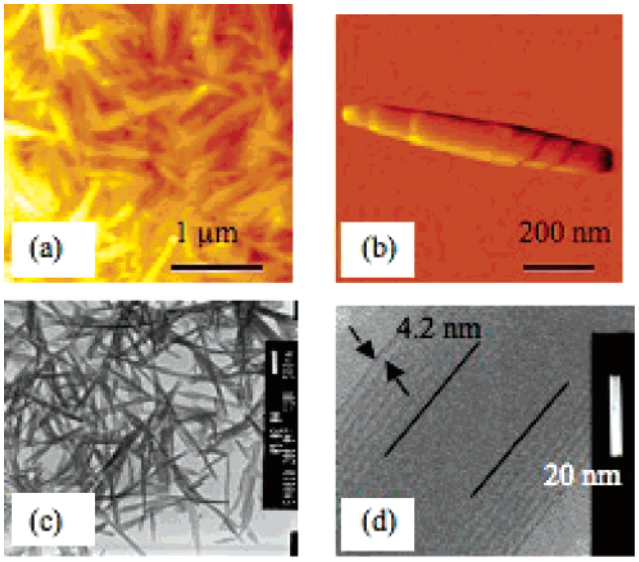

Figure 2. (a), (b) AFM images of C_3F_7-Azo^+-$K_4Nb_6O_{17}$ hybrid nanotubes. (c), (d) TEM and HRTEM image of C_3F_7-Azo^+-$K_4Nb_6O_{17}$ hybrid nanotubes.

The X-ray diffraction patterns of C_3F_7-Azo^+-$K_4Nb_6O_{17}$ are shown in Figure 1c, together with MV^{2+}-$K_4Nb_6O_{17}$ (Figure 1b) and $K_4Nb_6O_{17}$·$3H_2O$ (Figure 1a). The (0*k*0) reflection peaks showed marked changes after the guest−guest ion exchange, while keeping the whole profiles of the reflection patterns unchanged. The 2θ angle of the (020) diffraction peaks of MV^{2+}-$K_4Nb_6O_{17}$ and C_3F_7-Azo^+-$K_4Nb_6O_{17}$ were smaller than that of the untreated $K_4Nb_6O_{17}$·$3H_2O$. These observations confirm that the interlayer spacings of $K_4Nb_6O_{17}$·$3H_2O$ topochemically expand from the starting 1.88 nm to 2.26 and 4.20 nm by its reaction with MV^{2+} and C_3F_7-Azo^+, respectively. The d_{020} values corresponding to the sum of two adjacent interlayer spacings are regarded as the basal spacing. The adjacent two interlayers are different from each other due to the adsorption of guest molecules situating only in interlayer I. The interlayer expansion was determined to be 2.97 nm by subtracting the sum of thickness of the interlayer II and niobate layer of $K_4Nb_6O_{17}$·$3H_2O$ (1.23 nm) from the observed basal spacing (4.20 nm).[10] Considering the interlayer spacings and the size of the guest molecules (2.03 nm length), it is postulated here that C_3F_7-Azo^+ forms bilayer coverage with its long molecular axis being inclined to the niobate sheet.

The AFM image of the MV^{2+}-$K_4Nb_6O_{17}$ hybrid can be seen (see Supporting Information). The surface morphology of the MV^{2+}-$K_4Nb_6O_{17}$ hybrid shows the sheets layer-by-layer restacking. The important information obtained from AFM was the height image indicating the basal spacing of the MV^{2+}-$K_4Nb_6O_{17}$ hybrid. It corresponds well with the X-ray diffraction data. The AFM (Figure 2a,b), TEM, and HRTEM images (Figure 2c,d) of the C_3F_7-Azo^+-$K_4Nb_6O_{17}$ hybrid clearly show the tubular nature of the nanostructure. The AFM image (Figure 2b) shows a typical multilayered nanotube of C_3F_7-Azo^+-$K_4Nb_6O_{17}$ (ca. 1000 nm × 100 nm), where the niobate sheet is rolled up to form a four-layer spiral nanotube. All the samples in the AFM images have the tubular structure, and no hybrid sheet type structures are observed. This indicates that the spiral nanotube formation from exfoliated nanosheets are almost quantitative under the preparation conditions. The HRTEM image (Figure 2d) clearly indicates the formation of the multilayered nanotube with the interlayer distance of 4.2 nm. The nanotube has a hollow with a diameter of ca. 30 nm. From these images, we can readily see that the C_3F_7-Azo^+-$K_4Nb_6O_{17}$ hybrid has a multilayer tubular structure. The interlayer spacing of the obtained multilayer nanotubes (4.2 nm) corresponds well with the X-ray diffraction data (Figure 1c). This observation strongly suggests that, unlike carbon nanotubes, the C_3F_7-Azo^+-$K_4Nb_6O_{17}$ hybrid nanotubes have a multilayer spiral nanotube structure.

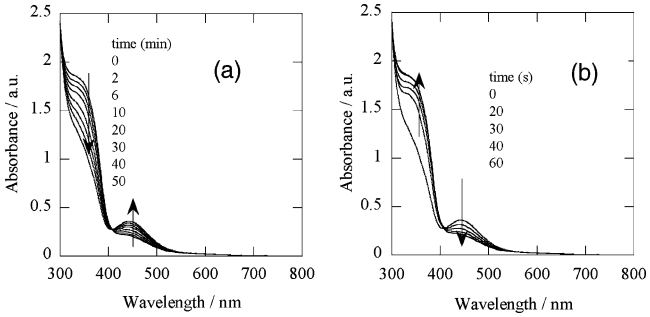

Figure 3. UV−Visible spectral changes of (a) C_3F_7-Azo^+-$K_4Nb_6O_{17}$ hybrid nanotubes on 365-nm irradiation (2.45 mW/cm^2), and (b) C_3F_7-Azo^+-$K_4Nb_6O_{17}$ hybrid nanotubes on 458-nm irradiation (8.10 mW/cm^2).

Figure 3 shows the change in the absorption spectra of the C_3F_7-Azo^+-$K_4Nb_6O_{17}$ nanotubes upon UV light (365 nm, 2.45 mW/cm^2) irradiation. After UV irradiation, the band due to the trans isomer (at around 357 nm) decreased (the spectrum in Figure 3a was recorded after 50 min UV irradiation, indicating trans-to-cis isomerization. UV irradiation for a longer period did not cause a further spectral change. The absorption band ascribable to the cis isomer appeared at 449 nm. The 449 peak is ascribed to the n-π^* transition of the cis isomer. Upon visible light (458 nm, 8.10 mW/cm^2) irradiation, the absorption spectrum almost recovered to the starting one (Figure 3b shows the absorption spectrum recorded after visible light irradiation). Obviously, the cis-to-trans isomerization was much more reactive than the trans-to-cis conversion. The reversible spectral change could be repeated many times over.

Supporting Information Available: Synthesis of C_3F_7-Azo^+Br, a typical SEM image of the $K_4Nb_6O_{17}$·$3H_2O$, and the AFM image of the MV^{2+}-$K_4Nb_6O_{17}$ hybrid. This material is available free of charge via the Internet at http://pubs.acs.org.

References

(1) (a) Iijima, S. *Nature* **1991**, *354*, 56. (b) Hu, J.; Odom, T. W.; Lieber, C. M. *Acc. Chem. Res.* **1999**, *32*, 435. (c) Dai, H. *Acc. Chem. Res.* **2002**, *35*, 1035. (d) Mitchell, D. T.; Lee, S. D.; Trofin, L.; Li, N.; Nevanen, T. K.; Soderlund, H.; Martin, C. R. *J. Am. Chem. Soc.* **2002**, *124*, 11864. (e) Shimizu, T.; Masuda, M.; Minamikawa, H. *Chem. Rev.* **2005**, *105*, 1401.
(2) (a) Chen, C. C.; Yeh, C. C. *Adv. Mater.* **2000**, *12*, 738. (b) Peng, X. G.; Manna, L.; Yang, W. D.; Wickham, J.; Scher, E.; Kadavanich, A.; Alivisatos, A. P. *Nature* **2000**, *404*, 59.
(3) (a) Lakshmi, B. B.; Patrissi, C. J.; Martin, C. R. *Chem. Mater.* **1997**, *9*, 2544. (b) Hoyer, P. *Langmuir* **1996**, *12*, 1411. (c) Zelenski, C. M.; Dorhout, P. K. *J. Am. Chem. Soc.* **1998**, *120*, 734.
(4) (a) Goldberger, J.; He, R.; Zhang, Y.; Lee, S.; Yan, H.; Choi, H.; Yang, P. *Nature* **2003**, *422*, 599. (b) Tenne, R.; Margulis, L.; Genut, M.; Hodes, G. *Nature* **1992**, *360*, 444. (c) Feldman, Y.; Wasserman, E.; Srolovits, D. J.; Tenne, R. *Science* **1995**, *267*, 222.
(5) (a) Saupe, G. B.; Waraksa, C. C.; Kim, H. N.; Han, Y. J.; Kaschak, D. M.; Skinner, D. M.; Mallouk, T. E. *Chem. Mater.* **2000**, *12*, 1556. (b) Du, G.; Chen, Q.; Yu, Y.; Zhang, S.; Zhu, W.; Peng, L. M. *J. Mater. Chem.* **2004**, *14*, 1437.
(6) (a) Horvath, I. T.; Rabai, J. *Science* **1994**, *266*, 72. (b) Myers, K. E.; Kumer, K. *J. Am. Chem. Soc.* **2000**, *122*, 12025. (c) Kameo, Y.; Takahashi, S.; Kowald, M. K.; Ohmachi, T.; Takagi, S.; Inoue, H. *J. Phys. Chem. B* **1999**, *103*, 9562.
(7) (a) Yui, T.; Yoshida, H.; Tachibana, H.; Tryk, D. A.; Inoue, H. *Langmuir* **2002**, *18*, 891. (b) Yui, T.; Uppili, S. R.; Shimada, T.; Tryk, D. A.; Yoshida, H.; Inoue, H. *Langmuir* **2002**, *18*, 4232. (c) Lucia, L. A.; Yui, T.; Sasai, R.; Takagi, S.; Takagi, K.; Yoshida, H.; Whitten, D. G.; Inoue, H. *J. Phys. Chem. B* **2003**, *107*, 3789.
(8) Gesperin, M.; Bihan, M.-T. L. *J. Solid State Chem.* **1982**, *43*, 346.
(9) Nassau, K.; Shiever, J. W.; Bernstein, J. L. *J. Electrochem. Soc.* **1969**, *116*, 348.
(10) Kinomura, N.; Kumada, N.; Muto, F. *J. Chem. Soc., Dalton Trans.* **1985**, 2349.

JA0564564